IEEE Access
Multidisciplinary ⋮ Rapid Review ⋮ Open Access Journal

Received December 4, 2020, accepted December 19, 2020, date of publication December 22, 2020,
date of current version December 31, 2020.

Digital Object Identifier 10.1109/ACCESS.2020.3046532

Comprehensive Analysis of the Impact of the TCSC on Distance Relays in Interconnected Transmission Networks

DOAA KHALIL IBRAHIM[1], (Senior Member, IEEE), GHADA M. ABO-HAMAD[1], ESSAM EL-DIN M. ABOUL ZAHAB[1], AND AHMED F. ZOBAA[2], (Senior Member, IEEE)

[1]Department of Electrical Power Engineering, Faculty of Engineering, Cairo University, Giza 12613, Egypt
[2]College of Engineering, Design and Physical Sciences, Brunel University London, Uxbridge UB8 3PH, U.K.

Corresponding author: Doaa Khalil Ibrahim (doaakhalil73@eng.cu.edu.eg)

ABSTRACT This article extensively investigates the calculations of the compensation factor of the thyristor-controlled series compensator (TCSC), which are used to accurately evaluate the negative impacts of the TCSC on the performance of conventional distance relays. To broadly evaluate the distance protection performance, the TCSC was adapted to the IEEE 9-bus system as one of the interconnected transmission networks that are increasingly spreading to improve service reliability, reduce reserve capacity, and enhance system efficiency. In addition, IEEE 39-bus system, as a large interconnected system, is also examined to generalize the TCSC impact on different interconnected systems. To determine the precise impact, the impedance of the TCSC was calculated based on its practical design parameters. The impedance of the TCSC was examined as a function of transmission line impedance and firing angle. Both Mho and Quadrilateral distance relays were tested using the MATLAB/Simulink environment for different types of faults, fault locations, fault resistances, and firing angles for capacitive, inductive, and blocking modes of TCSC operation. In addition, distance relay performance was evaluated during power swing phenomenon in the presence of the TCSC. Simulation tests indicated the negative impacts of the TCSC on distance relay operation, which are not limited to over-reach and under-reach in faulty conditions but also to maloperation in dynamic disturbances that cause power swing phenomena on the protected line.

INDEX TERMS Distance relays, interconnected transmission networks, over-reach and under-reach, power swing, thyristor-controlled series compensator (TCSC).

I. INTRODUCTION

The philosophy of flexible alternating-current transmission systems (FACTS) is to control power flow in transmission lines, enhance power system stability, reduce line losses and voltage control achievement based on power electronics. FACTS controllers can be mainly categorized as variable impedance controllers and voltage source converter controllers [1]. The thyristor-controlled series compensator (TCSC), which belongs to the variable impedance type of controllers, offers many advantages in power systems, such as fast and continuous control of the transmission line series compensation level, suppression of the active power oscillations, elimination of sub-synchronous oscillations, and voltage support [2].

On the other hand, the presence of the TCSC in the fault loop has a negative impact on the steady-state and transient voltage and fault current components due to the variable capacitive impedance or inductive impedance in series with the protected line. It affects the impedance measured by distance relay and accordingly leads to under-reach or over-reach problems [3]–[9]. The performance of the distance relay in the presence of the TCSC has been discussed in several published studies such as [3]–[5]. Most of the demonstrated results are based on the impedance estimated by the distance relay without considering the calculations of TCSC impedance. The reported results indicate false trips for the faults behind the TCSC on the protected and adjacent

The associate editor coordinating the review of this manuscript and approving it for publication was Zhigang Liu.

transmission lines. The techniques introduced in [4], [5] mitigate these errors by modifying the communication-aided schemes. However, the test results have pointed out some concerns, such as the delayed tripping time for internal faults, tripping of the adjacent line for internal faults in the case of channel breakdown, and the lack of monitoring for the communication channel during unfaulty system operation. In [6], the distance relay behavior in the presence of TCSC is investigated. The achieved results ensured that the existence of TCSC at the near end of the next line greatly affects the relay to overreaching, considering or neglecting MOV operation, but the analysis did not consider TCSC practical parameters that may affect the accuracy of results. In addition, the evaluation of distance relay due to fault location and fault types is not investigated in the achieved results. The error in the distance relay performance due to the presence of the TCSC is also reviewed in [7], meanwhile the study did not consider TCSC practical modelling and the results have just been restricted to three phase faults only.

TCSC impedance calculations, depending on synchronized data transferred from TCSC to relays, are studied in [8], [9]. The firing angle, updated by synchronized voltage control system, is used to calculate TCSC impedance as demonstrated in [8]. Under the studied TCSC control mode, a jumping point from maximum capacitive mode to maximum inductive mode exists during the gradual change of the conduction angle, however it does not occur practically as the smooth transition between inductive to capacitive modes is not allowed. Another study for TCSC effects on the impedances seen by distance relays is presented in [9] under a variety of loading conditions based on load flow studies using Newton-Raphson method.

Considering the investment savings and technical benefits, the interest in interconnected transmission networks has been growing worldwide [10]. Nevertheless, the protection of such systems is not as simple as that of double-ended systems since the impact of faults occurring in each local subsystem may extent through the physical interconnections to neighboring subsystems, disturbing the system performance or even leading to false tripping, which imposes serious challenges for protection systems [11]. As known, the removal of a fault or a sudden load change in any line in an interconnected network affect the phase angle between the generated voltages. During such disturbances, the rotor of the generator swings around the final steady-state value, which results in a change in the current flowing through the line in the form of power swings [12]. Provided that the phase angle between the generated voltages continues changing, the apparent impedance measured by the relay during power swings may falsely appear like a fault. Thus, distance relays may face serious challenges in interconnected transmission networks under power swing phenomenon and especially in the presence of the TCSC. Few efforts have been exerted to evaluate distance relays for faults under power swing phenomenon in the presence of the TCSC such as the study in [13] that only covered capacitive mode of operation within a 30% to 40% compensation level.

We believe that there is still a need to assess the performance of the distance relay for the TCSC compensated lines in interconnected transmission networks covering all fault types and all modes of operation. Therefore, the target of this paper was to derive a simple and accurate expression of the compensation factor based on the practical design of TCSC parameters that are used to calculate the impedance of the TCSC. This expression is simply calculated and helps in the accurate assessment of the distance relay performance for interconnected transmission networks possessing the TCSC. Mho/Quadrilateral distance relays, as impedance-based protection, are modelled under both normal operating and faulty operating conditions at different firing angles, fault types, and fault locations. Also, power swing conditions resulting from different fault types and under either TCSC modes of operation have been studied. The simulation studies were carried out on both IEEE 9-bus and IEEE 39-bus interconnected transmission systems. The results demonstrate that the TCSC negatively affects the distance relay decision for faults on the compensated lines. The difficulties in the performance of distance relays are not only over-reaching or under-reaching, but in some cases the fault is not even detected by both Mho/Quadrilateral characteristics.

This rest of this paper is arranged as follows. Section II shows concisely the TCSC structure and the operating principles, while in Section III, the TCSC impedance calculation principle is presented. Section IV describes how TCSC is applied for IEEE 9-bus system, and how its reactance changes with firing angle. The extensive results for evaluating the impact of the TCSC on Mho and Quadrilateral relays performance in IEEE 9-bus system are offered in Section V and Section VI respectively. Further performance evaluation for Mho/Quadrilateral relays is carried out on IEEE 39-bus system as a large system as presented in Section VII. Lastly, the conclusions are drawn in Section VIII.

II. STRUCTURE AND OPERATION OF THYRISTOR-CONTROLLED SERIES COMPENSATOR (TCSC)

The TCSC practical module, with its protective elements, is shown in Fig. 1. It comprises a series capacitor, C, in parallel with a thyristor-controlled reactor (TCR), Ls, Ultra-High Speed Contact (UHSC) across the valves, is used to minimize the conduction losses when the TCSC valves are fully "on" for prolonged mode operation. A metal-oxide varistor (MOV) as a nonlinear resistor is connected across the series capacitor to avoid high overvoltage. In addition, a circuit breaker (CB) is installed across the capacitor for controlling its inclusion in the line as the CB bypasses the capacitor when a severe fault or equipment malfunction event occurs. A current-limiting inductor, Ld, is inserted in the circuit to limit both the magnitude and the frequency of the capacitor current during bypass operation [1].

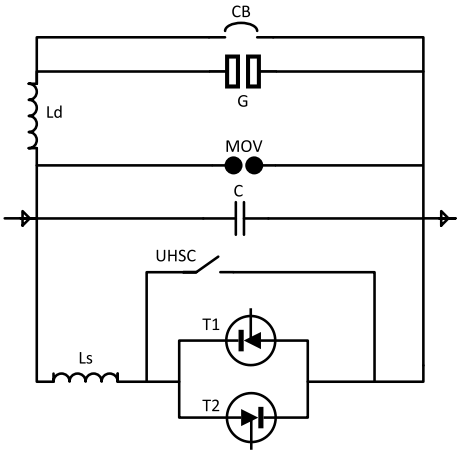

FIGURE 1. Thyristor-controlled series compensator (TCSC) module.

During faulty conditions, the operational modes of the TCSC can be categorized as follows [14]–[17]: bypass mode without MOV, capacitive boost mode with/without MOV, inductive boost mode with/without MOV, and thyristor blocked mode.

For low-impedance faults with high currents, both the MOV and TCR act and the TCSC operates in bypass mode; thus, the overall impedance calculated by the distance relay increases beyond the real value, which causes relay under-reaching.

For high-impedance faults, the capacitor voltage is less than the protective voltage level of the MOV; the capacitive boost mode without MOV is operated. Accordingly, for these faults, the MOV is not activated and the fault current passes through the capacitor. For that state, the distance relay estimates an impedance value that is smaller than the real impedance, which results in relay overreaching.

During the capacitive boost mode with the MOV, the MOV conducts partially for faults, resulting in moderate values of the fault current. For that case, the overall impedance is the equivalent parallel combination of the capacitor and the MOV, at which the relay also overreaches but differs from the prior case.

Due to the overcurrent of the capacitor and thyristors that is caused by thyristor firing angle fluctuation due to the abrupt variation in capacitor voltage phase, the firing of the TCR would stop and TCSC would operate in blocked mode. In this situation, the circuit works as a static capacitor and the relay also overreaches, but less than the capacitor boost mode [3].

Consequently, based on the impedance introduced by the TCSC, three different working regions for the TCSC can occur: the inductive region, resonance region, and capacitive region. A smooth transition from the inductive to capacitive mode is prohibited since there is a resonant region between them.

III. TCSC IMPEDANCE CALCULATION BASED ON COMPENSATION FACTOR CALCULATION

Considering that the equivalent circuit of the TCSC is modelled as a capacitor connected in parallel with a variable inductor, as illustrated in Fig. 2, the TCSC impedance (Z_{TCSC}) is expressed by the following equation, where X_C is the capacitive reactance and $X_L(\alpha)$ is the branch inductive reactance, which is function of firing angle (α) and $X_C < X_L(\alpha) < \infty$ [17]:

$$Z_{TCSC}(\alpha) = \frac{(X_C.X_L(\alpha))}{(X_L(\alpha) - X_C)} = \frac{(X_C)}{(1 - (X_C/X_L(\alpha))} \quad (1)$$

In fact, the thyristor ratings determine the maximum limit of the TCSC impedance for the inductive operation by the TCSC compensation factor (ψ), while the capacitive reactance, X_C, of the TCSC is a function of transmission line impedance, where $X_C = K_C.Z_m$ (K_C is the capacitive compensation factor and Z_m is the transmission line impedance) [14].

By varying the firing angle (α), the inductor reactance, $X_{Ls}(\omega_0.Ls)$, changes to $X_L(\alpha)$ by applying the firing angle factor, $\Re(\alpha)$, as follows:

$$X_L(\alpha) = X_{Ls}\left(\frac{\pi}{(\pi - 2\alpha - \sin 2\alpha)}\right) = X_{Ls}.\mathrm{R}(\alpha) \quad (2)$$

The resonance factor (λ) can be estimated from (3), where ω_r and ω_0 are the resonance frequency and power frequency, respectively [18].

$$\text{Resonance factor } (\lambda) = \frac{\omega_r}{\omega_0} = \sqrt{\frac{X_C}{X_{Ls}}} \quad (3)$$

By substituting from (2) and (3) in (1), the TCSC impedance as a function of transmission line impedance and the TCSC compensation factor (ψ) can be expressed by the following:

$$Z_{TCSC}(\alpha) = \psi.Z_m \quad (4)$$

where ψ can be defined by the following:

$$\psi = -\frac{K_C}{(1 - \frac{\lambda^2}{\mathrm{R}(\alpha)})} \quad (5)$$

Based on the practical requirements and the thermal rating of X_{Ls} and X_C, the selection of the TCSC parameters has been considered here, as discussed in [18]. The minimum series compensation, K_C, determines the capacitor reactance at $\alpha = 90°$. The reactor size choice is significantly critical as X_{Ls} must be smaller than X_C. The ratio between X_{Ls} and X_C affects TCSC operating area. This ratio has to be less than one, but if X_{Ls}/X_C is less than 0.1, more than one resonance region will exist that leads to TCSC operating region restriction. Besides, if this ratio is more than 0.3, the TCSC compensation degree decreases, so the benefit from using TCSC will be limited. Typically, this ratio is between 0.1 and 0.3.

The resonance frequency, ω_r, must be far enough from the harmonics of the power frequency, ω_o. Therefore, in this research, based on the TCSC requirements and the analytical study of the simulated system, K_C was chosen to be 40% of the line impedance, and the ratio between the reactance of the inductor, X_{Ls}, and the capacitive reactance, X_C, was set

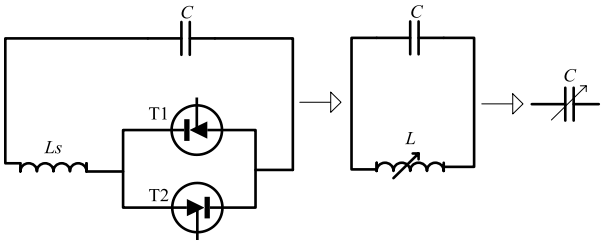

FIGURE 2. TCSC equivalent circuit.

by 0.2 which leads λ to be 2.23. Actually, these parameters can provide the best stable operation of the TCSC because of the wider operation in the capacitive area, the single region of resonance frequencies, the controllability, and the precision of the TCSC compensation.

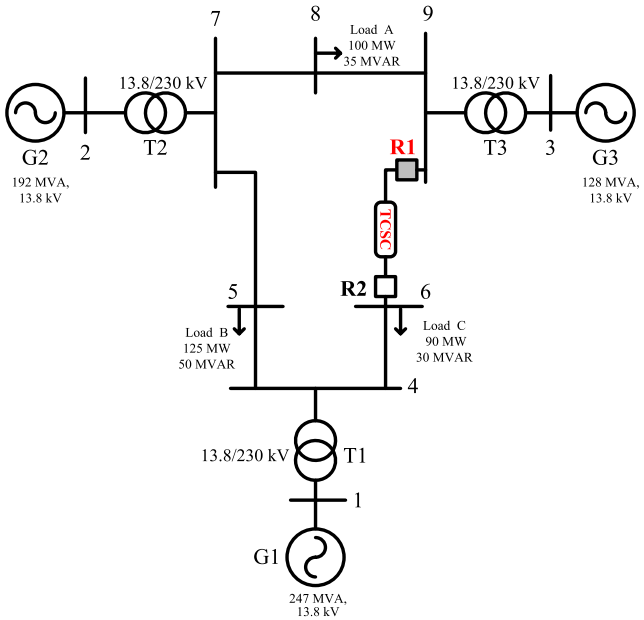

FIGURE 3. Tested IEEE 9-bus system.

IV. APPLYING TCSC FOR IEEE 9-BUS SYSTEM

In Fig. 3, the single line diagram of the IEEE 9-bus system is presented. The tested IEEE 9-bus system, as an interconnected system, is a common template for power flow and dynamic simulation studies for engineers and researchers to study system stability and to test different suggested algorithms and techniques. This system is composed of 3 loads, 3 transformers, and 3 generators/machines, which are interconnected through a network of 9 buses. The total generated power is 319.6 MW, while the total supplied load is 315 MW of active power and 115 MVAR of reactive power [19].

The TCSC was connected at the mid-point between buses 9 and 6, as recommended from the transient stability improvement point of view discussed in [20],[21] where the transmission line connecting buses 9 and 6 has a total length of 100 km.

The modelled TCSC, depending on the implementation of practical design parameters, can operate in capacitive or inductive mode under different firing angles. The resonance for the TCSC is about a 45° firing angle; therefore, the operation is forbidden in the range of 40–55°. The capacitive mode is attained with firing angles of 5–90°, where the TCSC impedance value is approximately 65.1–35.90 Ω and, accordingly, this range can achieve series compensation around 40–72% to avoid overcompensating, as discussed in [17]. The inductive mode relates to the firing angles between 0° and 40°, and the lowest impedance is at 0°. In the inductive operational mode, the TCSC impedance ranges between 8.79 and 64.11 Ω.

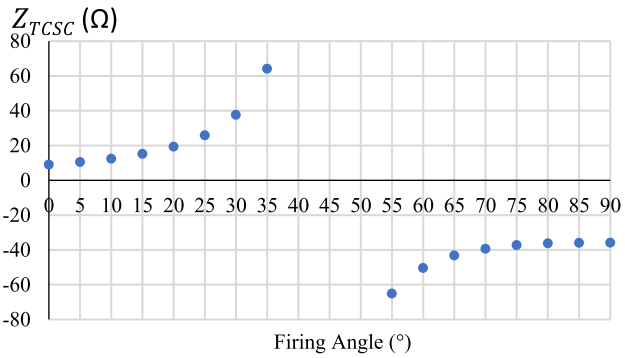

FIGURE 4. Characteristic curve of the fundamental frequency reactance of the TCSC.

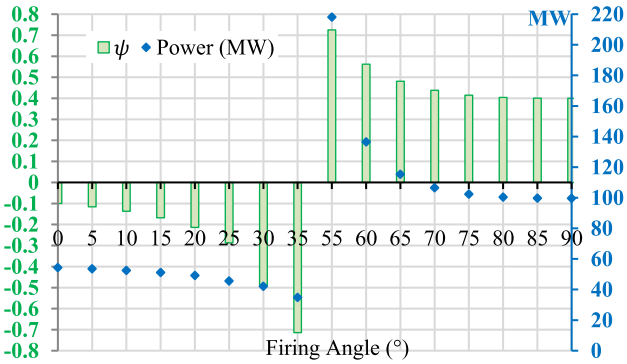

FIGURE 5. Power flow and compensation factor for the TCSC compensated line between buses 9 and 6 due to firing angle variation.

The fundamental frequency reactance of the TCSC is illustrated in Fig. 4 as a function of the firing angle. As per the analytical study, the maximum power transmitted by the line between buses 9 and 6 without the TCSC is 59.80 MW. If the TCSC is located in the middle, the transmitted power and the compensation factor will be as shown in Fig. 5, with variation in the firing angle. As illustrated, the maximum power transmitted can be achieved at $\alpha = 55°$, which corresponds to 218 MW, while the minimum transmitted power is 34 MW at $\alpha = 35°$.

V. MHO RELAY PERFORMANCE EVALUATION IN IEEE 9-BUS TEST SYSTEM

Regarding the distance protection performance on the TCSC compensated line in IEEE 9-bus system (between buses 9 and); the behavior of distance relay R1 will be investigated

TABLE 1. Performance Evaluation of R1 Mho relay for the compensated line between buses 9 and 6 in IEEE 9-bus system.

Fault Type	Fault Location	Inductive Mode			Capacitive Mode		Blocking Mode
		α=10°	α=20°	α=35°	α=55°	α=75°	α=90°
SLG	51% in Zone 1 (d=0.51)	Correct	Correct	Under	Correct	Correct	Correct
L-L		Under	Correct	Not	Correct	Correct	Correct
2L-G		Correct	Correct	Under	Correct	Correct	Correct
3L-G		Correct	Under	Under	Correct	Correct	Correct
SLG	70% in Zone 1 (d=0.7)	Under	Under	Under	Correct	Correct	Correct
L-L		Under	Under	Under	Correct	Correct	Correct
2L-G		Under	Under	Under	Correct	Correct	Correct
3L-G		Under	Under	Under	Correct	Correct	Correct
SLG	110% in Zone 2 (d=1.1)	Under	Under	Under	Over	Over	Over
L-L		Under	Under	Not	Correct	Correct	Over
2L-G		Under	Not	Not	Over	Over	Over
3L-G		Under	Under	Not	Over	Over	Over
SLG	150% in Zone 3 (d=1.5)	Correct	Correct	Not	Correct	Correct	Over
L-L		Correct	Correct	Not	Correct	Correct	Over
2L-G		Not	Not	Not	Correct	Correct	Over
3L-G		Not	Not	Not	Over	Over	Over

in the following subsections. It is worth mentioning that testing R1 for faults that occur before the TCSC (from bus 9 to the TCSC location) is not presented since the relay behaves correctly for all fault types. In addition, the tests only consider R1 as the performance of R2 on the same protected line is similar to R1.

Consequently, R1 was extensively tested for different fault types (SLG, L-L, 2L-G, and 3L-G) and fault locations (51%, 70%, 110%, and 150%, where the location is modeled from the beginning of the compensated line at bus 9) for the three modes of operation (inductive, capacitive, and blocking modes) under different firing angles (10°, 20°, 35°, 55°, 75°, and 90°).

The settings of the tested Mho distance relay in different zones were selected as follows: 80% of the line impedance between buses 9 and 6 for Zone 1; 100% of the line impedance between buses 9 and 6, in addition to 20% of the line impedance between buses 6 and 4 for Zone 2; and finally, 100% of the line impedance between buses 9 and 6, in addition to 100% of the line impedance between buses 6 and 4 for Zone 3.

The results are summarized in Table 1, where ''Correct'' and ''Not'' denote ''correct tripping'' and ''fail to trip'' respectively, while ''Under'' and ''Over'' denote ''under-reach'' and ''over-reach'' respectively.

A. EFFECT OF FIRING ANGLE

As shown in Table 1, the distance relay, R1, under-reaches in most cases in inductive mode and over-reaches in capacitive mode. In addition, in some cases of inductive mode, especially at a high firing angle of 35° when the minimum power is transmitted via the protected line, the distance relay fails to detect and trip for faults in different zones.

B. EFFECT OF FAULT LOCATION

In fact, the apparent impedance estimated by the distance relay without the TCSC is a function of the fault position on the line per unit of protected transmission line length (d) and line impedance and can be determined by the following:

$$Z_{App} = d.Z_m \tag{6}$$

From (4) and (6), the apparent impedance upon insertion of the TCSC impedance (Z_{App_TCSC}) as a function of transmission line impedance can be expressed by the following:

$$Z_{App\_TCSC} = (\psi + d).Z_m \tag{7}$$

Thus, the following is obtained:

$$\frac{Z_{App_{TCSC}}}{Z_{App}} = \frac{\psi}{d} + 1 \tag{8}$$

The analytical study in Fig. 6 demonstrates the TCSC impedance behavior under different locations of single line-to-ground (SLG) faults. Theoretically, in capacitive mode, the faults in Zone 1 are correctly detected under all compensation degrees, but all cases in Zone 2 and Zone 3 are incorrectly overreached. For the inductive mode of operation, the under-reach problem is indicated in Zone 1 as the compensation degree increases. The simulation studies illustrated in Table 1 demonstrate that the distance relay faces serious problems in inductive mode compared to other modes of operation. As shown, in most cases the relay under-reaches or fails to detect and trip faults as well, especially in Zone 2 and Zone 3, as illustrated for faults at 110% and 150%, respectively.

C. EFFECT OF FAULT TYPES

As discussed before, different reported studies have checked the performance of distance relays for three phase faults, as in [6], [7]. On the contrary, all fault types were tested here for extensive evaluation under different firing angles and fault locations, as shown in Table 1. The achieved results indicate that the distance relay is more sensitive for the three-phase fault types compared to the other types of faults.

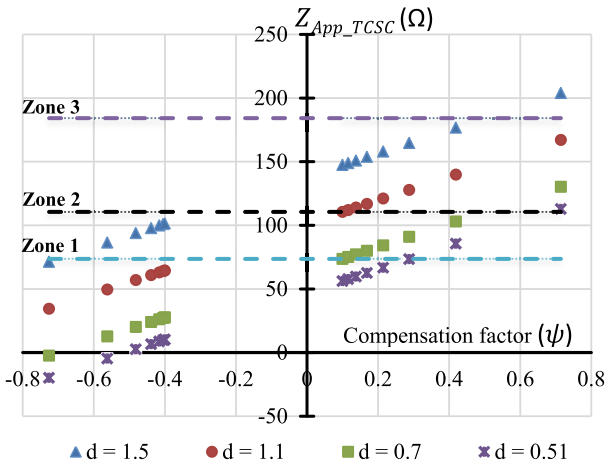

FIGURE 6. Apparent impedance with the TCSC for different compensation factors (ψ) and different locations (d) of SLG faults.

D. EFFECT OF FAULT RESISTANCE

Actually, the tabulated results in Table 1 show the performance of the distance relay for solid faults only. To achieve a comprehensive distance relay evaluation, tests were carried out for a wide range of fault resistances. As mentioned before, Zone 1 was considered to be 80% of the line impedance between buses 9 and 6; thus, the performance was investigated near the end of Zone 1. Accordingly, SLG faults are created at 60 km from bus 9 ($d = 0.6$), with fault resistance ranges from 10 Ω to 30 Ω at different firing angles.

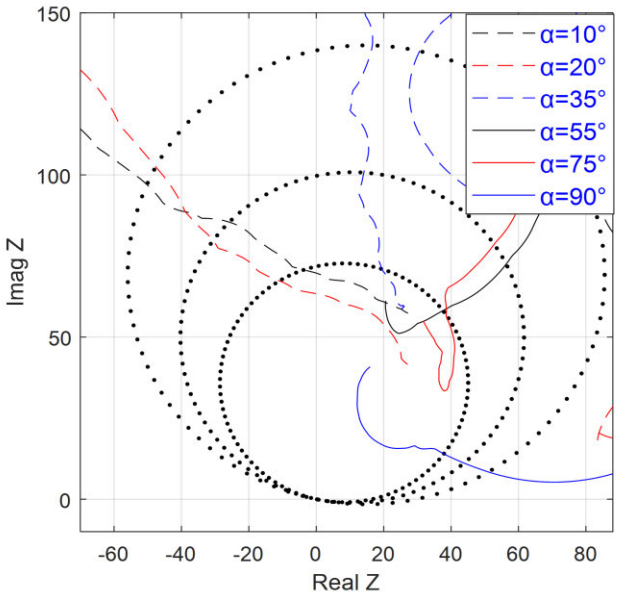

FIGURE 7. Apparent impedance of Mho relay for SLG fault at $d = 0.6$ with 10 ohm fault resistance.

The apparent impedance for the relay under a fault resistance of 10 Ω is demonstrated in Fig. 7. As indicated, the distance relay correctly detected the fault in Zone 1 for all

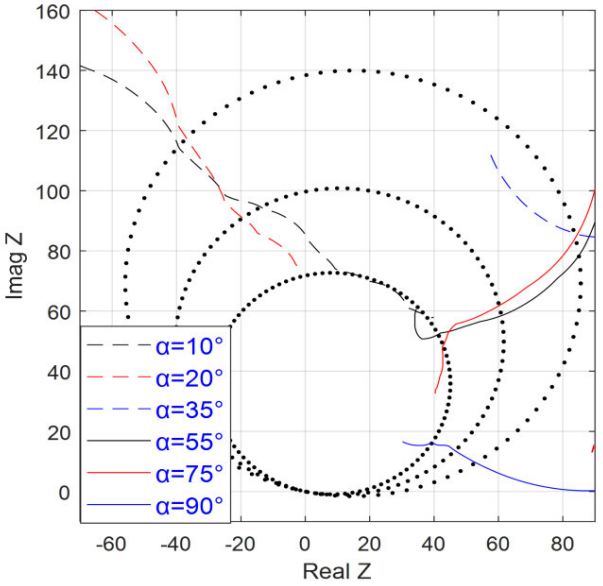

FIGURE 8. Apparent impedance of Mho relay for SLG fault at $d = 0.6$ with 20 ohm fault resistance.

firing angles. However, for a fault resistance of 20 Ω, as revealed in Fig. 8, the behavior changed. Under all cases of inductive mode, the distance relay under-reaches and detects the fault in Zone 2 for ($\alpha = 10°$ and 20°) and Zone 3 for the minimum transmitted power (as $\alpha = 35°$), while the fault was correctly detected in Zone 1 in all capacitive mode cases ($\alpha = 55°$, 75°, and 90°).

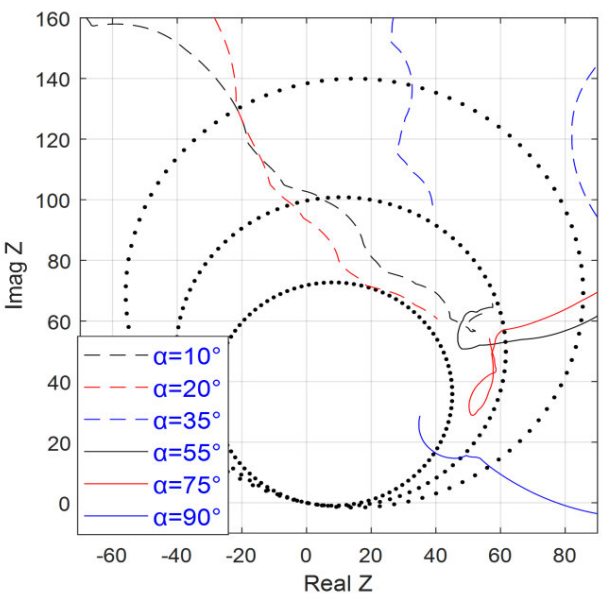

FIGURE 9. Apparent impedance of Mho relay for SLG fault at $d = 0.6$ with 30 ohm fault resistance.

In Fig. 9, for a fault resistance of 30 Ω, the tested fault cases were under-reached. This means that the fault resistance added in the faulted path was not compensated by the

impedance reduction introduced by the TCSC in capacitive mode, except for the only case of capacitive mode at $\alpha = 90°$, as the impedance is correctly seen in Zone 1.

If the fault resistance increases to 40 Ω, the distance relay fails to detect such faults for all modes of operation and under different firing angle values.

E. EFFECT OF POWER SWING

The evaluation of the distance relay was extended to cover its behavior during power swing phenomenon with the TCSC in both capacitive/inductive operation modes under different firing angles. As discussed in [22], the power swing phenomenon is modelled in the IEEE 9-bus test system by applying a solid three-phase fault or a SLG fault between buses 4 and 5 after 20 km from bus 4, and the faults take 20 cycles to be cleared from the fault initiation instant at 2 s, which causes power swing phenomenon.

Fig. 10 illustrates the voltages and current signals measured at R1 on bus 9 upon a three-fault occurrence between buses 4 and 5 at 2 s.

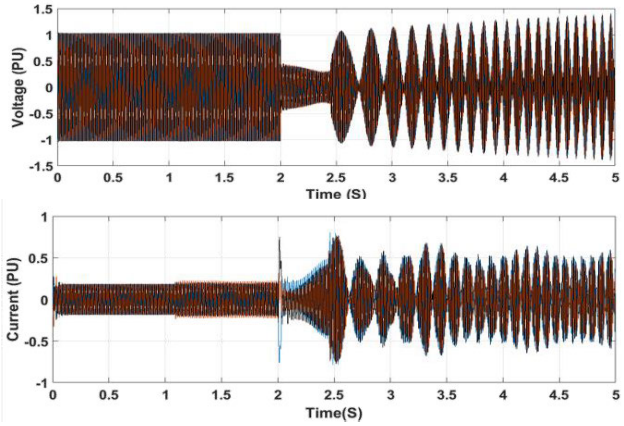

FIGURE 10. Voltages and current phasors at R1 on bus 9 upon three-fault occurrences between buses 4 and 5 at 2 s.

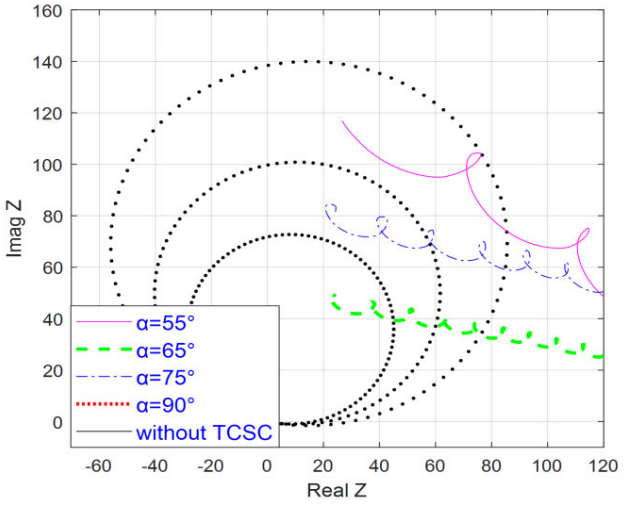

FIGURE 11. Apparent impedance of Mho relay under capacitive mode for power swing due to the SLG fault.

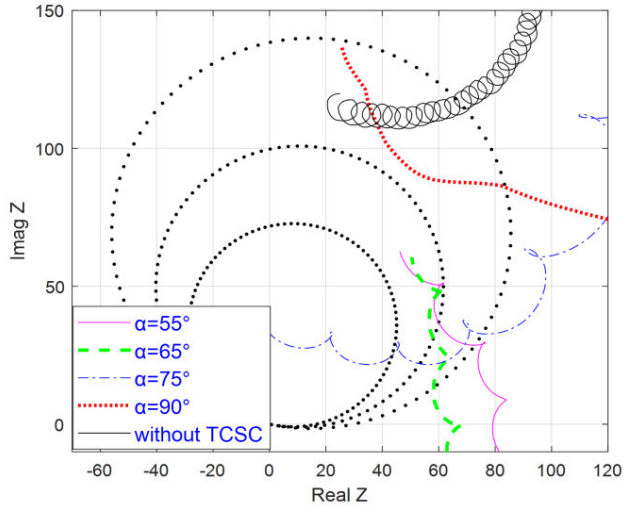

FIGURE 12. Apparent impedance of Mho relay under capacitive mode for power swing due to the three-phase fault.

1) IN CASE OF TCSC CAPACITIVE MODE

The trajectory impedance under power swing for capacitive mode due to a SLG fault on the line between buses 4 and 5 after 20 km from bus 4 is illustrated in Fig. 11. As revealed, the distance relay sees the power swing incorrectly as a fault for firing angles of 55°, 65°, and 75°, while for the cases without the TCSC and under a 90° firing angle, the impedance estimated by the relay is very far from the protected zone, which is not shown due to scale matters. Therefore, the relay is secure and does not trip correctly as no fault is detected in these cases.

On the other hand, due to a three-phase fault at the same location, the apparent impedance estimated by relay R1 is indicated in Fig. 12. It should be mentioned that the conventional distance relay, even in the case without the TCSC, falsely discriminates such a swing event as a fault in Zone 3, which needs a power swing blocking (PSB) function to be implemented to prevent such relay malfunction. For the TCSC compensated line, the distance relay behaves worse than the case without the TCSC as Fig. 12 ensures that the relay does not discriminate the swing case correctly and falsely trip for all firing angles. As shown, a nuisance tripping was issued at Zone 1 for $\alpha = 75°$ and Zone 2 for both $\alpha = 55°$ and 65° (approximately around the maximum transmitted power case), which increases the difficulties for dealing with power swing phenomenon.

2) IN CASE OF TCSC INDUCTIVE MODE

In Fig. 13 and 14, the apparent impedance of R1 for power swing due the SLG fault and the three-phase fault due to TCSC inductive mode are demonstrated. As shown, the relay behaves correctly and does not indicate any false trip action under the swing that occurs due to the SLG fault condition

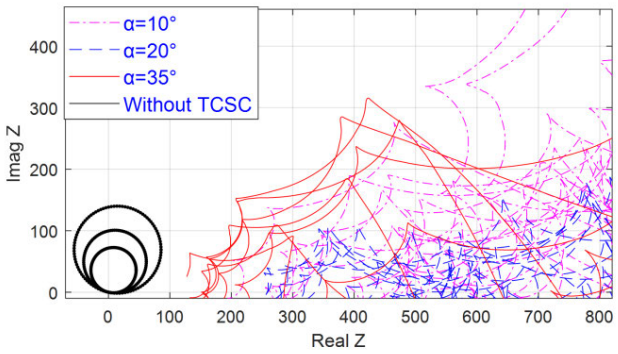

FIGURE 13. Apparent impedance of Mho relay under capacitive mode for power swing due to the SLG fault.

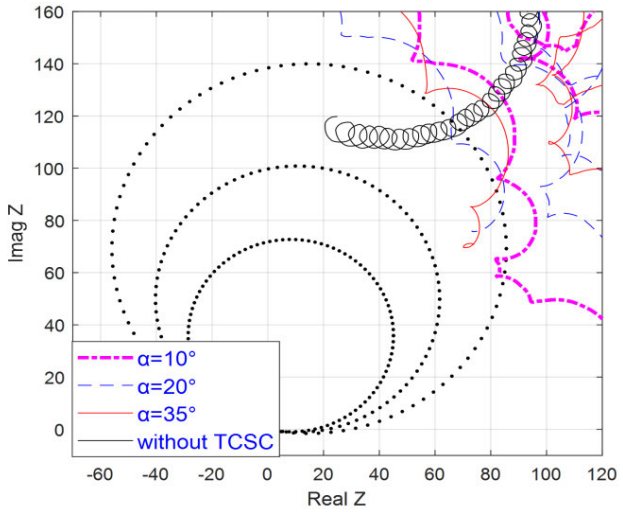

FIGURE 14. Apparent impedance of Mho relay under inductive mode for power swing due to the three-phase fault.

(Fig. 13). On the other hand, it indicates a false trip at Zone 3 for the swing that occurred due to three-phase fault cases for $\alpha = 20°$ and 35° but the case for $\alpha = 10°$, the distance relay behaves correctly as it does not falsely trip for this swing.

Although the TCSC can depress the power oscillations in transmission lines [2], the aforementioned results have indicated that the power swing has more influence on the performance of the distance relay, which protects the TCSC compensated line during capacitive mode rather than inductive mode. In addition, in some cases, the relay falsely discriminates the power swing as a fault in Zone 1 for $\alpha = 65°$ and 75° for a swing due to the SLG and three-phase fault, respectively, which means the relay will trip instantaneously in such cases.

VI. QUADRILATERAL RELAY PERFORMANCE EVALUATION IN IEEE 9-BUS TEST SYSTEM

Although that the Mho characteristic is simple to design and set, other distance relay characteristics have been developed to overcome Mho circle limitations. Quadrilateral relays, characterized by a trip region delimited by four lines, have been in use for several decades. Quadrilateral relays are desirable for their ability to give a better choice for protecting compensated lines; as their "reach" in the resistance and reactance directions can be independently controlled [23]. Accordingly, our study is extended to also evaluate the performance of Quadrilateral characteristic in the presence of TCSC. Therefore, R1 with a Quadrilateral characteristic (that protects the line between buses 9 and 6 in Fig. 3) was extensively examined for different fault types and fault locations for the three modes of operation under different firing angles. But, due to the limited space of the paper, only some cases are demonstrated. Such cases are selected to cover all zones of protection in addition that the Mho relay has faced serious difficulties to deal with them.

As per the results in Table 1, the worst cases were 3L-G faults at $\alpha = 35°$ and 75°, in addition to L-G fault under blocking mode at $\alpha = 90°$. Such cases are simulated at $d = 0.7$, 1.1, and 1.5 to investigate the Quadrilateral relay performance for all zones of the protected transmission line.

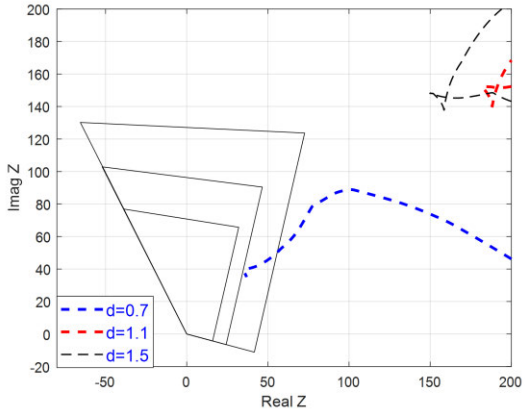

FIGURE 15. Apparent impedance of Quadrilateral relay for 3L-G fault at $\alpha = 35°$ for all zones of protection.

Fig. 15, shows the trajectory impedance for the Quadrilateral relay under 3L-G faults for $\alpha = 35°$. As shown, the performance was similar to Mho relay, as the Quadrilateral relay had also under-reached the fault in Zone 1 at $d = 0.7$, and did not act as a backup protection to detect Zone 2 and Zone 3 faults. However, the Quadrilateral relay behavior is slightly better than Mho relay for faults at $\alpha = 75°$ and 90°, as the relay correctly detects the faults at Zone 1, but over-reaches for the faults occurring at Zone 2 and Zone 3 as displayed in Fig. 16 and Fig. 17 respectively.

VII. FURTHER PERFORMANCE EVALUATION FOR MHO/QUADRILATERAL RELAYS ON IEEE 39-BUS SYSTEM

To validate TCSC modelling and ensure its negative impact on distance relays regardless the network configuration, further performance evaluation for Mho/Quadrilateral characteristics is carried out on IEEE-39 bus system as a larger interconnected system. IEEE-39 bus system, as shown

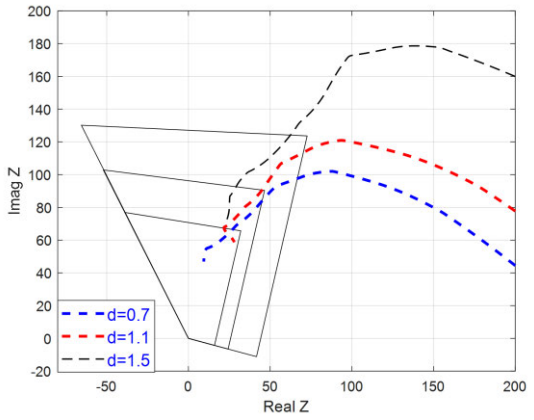

FIGURE 16. Apparent impedance of Quadrilateral relay for 3L-G fault at $\alpha = 75°$ for all zones of protection.

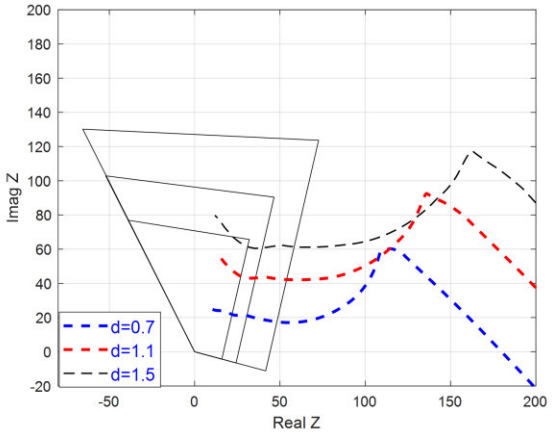

FIGURE 17. Apparent impedance of Quadrilateral relay for L-G fault at $\alpha = 90°$ for all zones of protection.

in Fig. 18, has 345, 230 and 22 kV buses, with 34 lines, 10 generators and 12 transformers [24].

The evaluation is carried out for the distance relay R1 that protects the line between buses 28 and 29 where the TCSC is placed at the mid-point of that line according to [25], [26]. Extensive tests are applied under different firing angles, fault types, fault locations and also power swing phenomenon. For six selective cases covering several firing angles under different conditions, Fig. 19 depicts the impedance trajectories monitored by R1 by using Quadrilateral or Mho characteristics.

For Case-1, that presents L-L fault in Zone 2 at $d = 0.9$ under $\alpha = 65°$, as illustrated both Mho and Quadrilateral relays are over-reached and detected the fault in Zone 1. In addition, both of them have under-reached for Case-2 when 2L-G fault is simulated at $d = 0.75$ in Zone 1 and under $\alpha = 15°$.

For Case 3 (L-G fault at $d = 0.9$ and under TCSC blocking mode of $\alpha = 90°$), the performance has changed. As demonstrated in Fig. 19, the Quadrilateral characteristic has correctly detected Case-3 while Mho relay has over-reached.

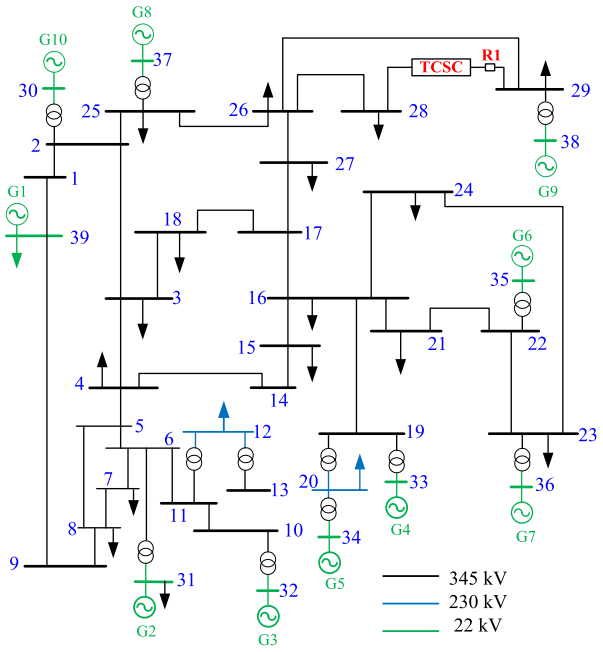

FIGURE 18. IEEE-39 bus system.

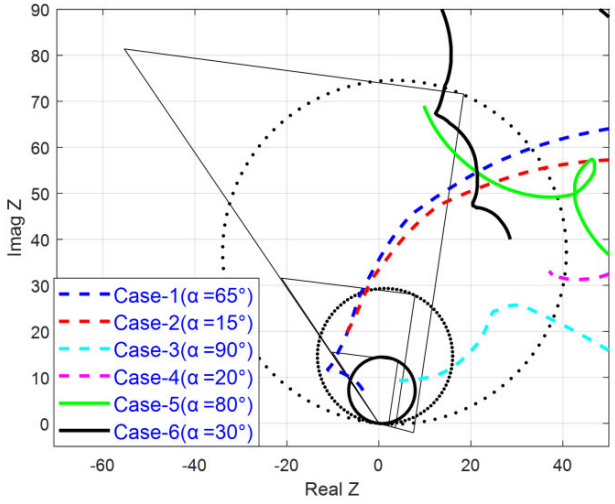

FIGURE 19. Apparent impedance of Mho/Quadrilateral relays for different tested cases on IEEE-39 bus system.

On the contrary, the response of both relays for Case 4 (3L-G fault at $d = 1.5$ under $\alpha = 20°$) ensures that the Mho relay correctly detected the fault in Zone 3 without any response from the Quadrilateral relay, that did not detect such fault.

The performance of both Quadrilateral and Mho relays during power swing phenomenon due to 3L-G on the line between 29-26 buses at $d = 0.8$ from bus 29 [27], is also investigated. Among the different carried out tests under different firing angles, the trajectory impedance for Case 5 and Case 6 under $\alpha = 80°, 30°$ respectively are shown in Fig. 19. As revealed from both cases, Mho and Quadrilateral relays have behaved incorrectly and detected such power swing event as a fault under Zone 3.

According to the achieved results, it can be deduced that TCSC affects the apparent impedance seen by both Mho and Quadrilateral relays and leads to errors in their decisions for different systems configurations.

VIII. CONCLUSION

A simple and accurate expression of the TCSC compensation factor (ψ) used for TCSC impedance calculations is presented. Such expression is based on the practical TCSC design parameters that can be calculated offline.

Based on the TCSC impedance calculations, a comprehensive analysis was carried out to determine the influence of the TCSC on both Mho/Quadrilateral distance relays. The study is applied on two interconnected IEEE benchmark systems, IEEE 9-bus system, and IEEE 39-bus system. The study was carried out by modelling the tested systems, TCSC, and distance relay (Mho & Quadrilateral characteristics) using the MATLAB simulator. For model validation, the distance relay was tested without the TCSC and ensured correct performance for different fault types and locations.

This study, which was done on such interconnected transmission networks, did not only investigate faulty conditions, but also examined more scenarios such as interruptions on other lines that cause power swing. The results indicate that introducing the TCSC in transmission lines has a noteworthy negative impact on the distance relay behavior for both Mho and Quadrilateral characteristics. The problem is not limited to under/over reach, but it also causes the distance relay to mal-operate in some cases and lose its reliability in other cases. Inductive mode has more serious negative impacts compared to capacitive mode in faulty cases on both characteristics of distance relays, especially at the minimum transmitted power, corresponding to $\alpha = 35°$ for all types of faults in Zone 2 and Zone 3. Also, inductive mode introduces poor behavior on the distance relay in the case of fault resistance as the fault impedance is added to its impedance, which reflects on the measured apparent impedance by the relay. It was also deduced that as ψ increases, the distance relay maloperation occurs. Although the TCSC in transmission lines introduces the effect of damping power oscillation, an effective blocking scheme is needed to be applied in the distance relay to overcome the incorrect behavior of the relay during power swing events, especially during capacitive mode since it may trip instantaneously in zone 1 not only in the small power systems but also in the large power systems.

The contributions of this comprehensive analysis can be summarized as follows:

- The analysis has considered practical TCSC design parameters.
- The tests have been done for both Mho and Quadrilateral characteristics.
- The tests have been carried out on different interconnected transmission networks.
- Extensive simulation tests are achieved to cover numerous cases under different fault locations, fault types, fault resistance, TCSC firing angles, as well as power swing phenomenon.

Therefore, the future work is to adapt distance relays to overcome the abovementioned problems for interconnected transmission networks based on the accurate calculations that introduce the TCSC into transmission lines.

REFERENCES

[1] R. M. Mathur and K. R. Varma, *Thyristor-Based FACTS Controllers for Electrical Transmission Systems*. Hoboken, NJ, USA: Wiley, 2002.
[2] K. R. Padiyar, *Facts Controllers in Power Transmission and Distribution*. Anshan, China: Technology & Engineering, 2009.
[3] T. S. Sidhu and M. Khederzadeh, "TCSC impact on communication-aided distance-protection schemes and its mitigation," *IEE Proc. Gener., Transmiss. Distrib.*, vol. 152, no. 5, pp. 714–728, Sep. 2005, doi: 10.1049/ip-gtd:20045261.
[4] M. Khederzadeh and T. S. Sidhu, "Impact of TCSC on the protection of transmission lines," *IEEE Trans. Power Del.*, vol. 21, no. 1, pp. 80–87, Jan. 2006, doi: 10.1109/TPWRD.2005.858798.
[5] T. S. Sidhu and M. Khederzadeh, "Series compensated line protection enhancement by modified pilot relaying schemes," *IEEE Trans. Power Del.*, vol. 21, no. 3, pp. 1191–1198, Jul. 2006, doi: 10.1109/TPWRD.2006.876982.
[6] A. Kazemi, S. Jamali, and H. Shateri, "Distance relay over-reaching in presence of TCSC on next line considering MOV operation," in *Proc. 45th Int. Universities Power Eng. Conf. UPEC*, Cardiff, Wales, Sep. 2010, pp. 1–6.
[7] S. Biswas and P. K. Nayak, "State-of-the-art on the protection of FACTS compensated high-voltage transmission lines: A review," *High Voltage*, vol. 3, no. 1, pp. 21–30, Mar. 2018, doi: 10.1049/hve.2017.0131.
[8] F. Wei, X. Lin, Z. Li, L. Chen, and M. S. Khalid, "A new distance protection method considering TCSC-FCL dynamic impedance characteristics," *IEEE Trans. Power Del.*, vol. 33, no. 3, pp. 1428–1437, Jun. 2018, doi: 10.1109/TPWRD.2017.2771276.
[9] J. Piri, G. Bandyopadhyay, and M. Sengupta, "Effects of including SVC and TCSC in an existing power system under normal operating condition a case study," in *Proc. IEEE Int. Conf. Power Electron., Drives Energy Syst. (PEDES)*, Dec. 2018, pp. 18–21, doi: 10.1109/PEDES.2018.8707541.
[10] P. K. Nayak, A. K. Pradhan, and P. Bajpai, "A three-terminal line protection_newline scheme immune to power swing," *IEEE Trans. Power Del.*, vol. 31, no. 3, pp. 999–1006, Jun. 2016, doi: 10.1109/TPWRD.2014.2387873.
[11] V. K. Gaur and B. Bhalja, "A new faulty section identification and fault localization technique for three-terminal transmission line," *Int. J. Electr. Power Energy Syst.*, vol. 93, pp. 216–227, Dec. 2017, doi: 10.1016/j.ijepes.2017.05.024.
[12] B. A. M. Alizadeh, M. Khederzadeh, and R. Razzaghi, "Fault detection during power swing in thyristor-controlled series capacitor-compensated transmission lines," *Electr. Power Syst. Res.*, vol. 187, Oct. 2020, Art. no. 106481, doi: 10.1016/j.epsr.2020.106481.
[13] S. Biswas and P. K. Nayak, "An unblocking assistance to distance relays protecting TCSC compensated transmission lines during power swing," *Int. Trans. Electr. Energy Syst.*, vol. 29, no. 8, Aug. 2019, , Art. no. e12034, doi: 10.1002/2050-7038.12034.
[14] N. G. Hingorani and L. Gyugyi, *Understanding FACTS: Concepts and Technology of Flexible AC Transmission Systems*. New York, NY, USA: IEEE Press, 2000.
[15] J. Urbanek, R. J. Piwko, E. V. Larsen, B. L. Damsky, B. C. Furumasu, W. Mittlestadt, and J. D. Eden, "Thyristor controlled series compensation prototype installation at the slatt 500 kV substation," *IEEE Trans. Power Del.*, vol. 8, no. 3, pp. 1460–1469, Jul. 1993, doi: 10.1109/61.252673.
[16] G. G. Karady, T. H. Ortmeyer, B. R. Pilvelait, and D. Maratukulam, "Continuously regulated series capacitor," *IEEE Trans. Power Del.*, vol. 8, no. 3, pp. 1348–1355, Jul. 1993, doi: 10.1109/61.252661.
[17] S. M. R. Slochanal, M. Saravanan, and A. C. Devi, "Application of PSO technique to find optimal settings of TCSC for static security enhancement considering installation cost," in *Proc. Int. Power Eng. Conf.*, Dec. 2005, pp. 1–394, doi: 10.1109/IPEC.2005.206940.
[18] A. D. Del Rosso, C. A. Canizares, and V. M. Dona, "A study of TCSC controller design for power system stability improvement," *IEEE Trans. Power Syst.*, vol. 18, no. 4, pp. 1487–1496, Nov. 2003, doi: 10.1109/TPWRS.2003.818703.

[19] A. Halder, N. Pal, and D. Mondal, "Transient stability analysis of a multimachine power system with TCSC controller—A zero dynamic design approach," *Int. J. Electr. Power Energy Syst.*, vol. 97, pp. 51–71, Apr. 2018, doi: 10.1016/j.ijepes.2017.10.030.

[20] M. Abapour, P. Aliasghari, and M.-R. Haghifam, "Risk-based placement of TCSC for transient stability enhancement," *IET Gener., Transmiss. Distrib.*, vol. 10, no. 13, pp. 3296–3303, Oct. 2016, doi: 10.1049/iet-gtd.2016.0170.

[21] W. S. Sakr, R. A. El-Sehiemy, and A. M. Azmy, "Optimal allocation of TCSCs by adaptive DE algorithm," *IET Gener., Transmiss. Distrib.*, vol. 10, no. 15, pp. 3844–3854, Nov. 2016, doi: 10.1049/iet-gtd.2016.0362.

[22] H. Fasihipour and S. Seyedtabaii, "Fault detection and faulty phase(s) identification in TCSC compensated transmission lines," *IET Gener., Transmiss. Distrib.*, vol. 14, no. 6, pp. 1042–1050, Mar. 2020, doi: 10.1049/iet-gtd.2019.1019.

[23] D. A. Tziouvaras, S. R. Chano, J.-L. Chanelière, J. Holbach, S. Moroni, M. S. Sachdev, C. E. Zavolas, S. J. Lee, and G. H. Topham, *Modern Distance Protection Functions and Applications*. Paris, France: CIGRE Publications, Oct. 2008.

[24] K. R. Padiyar, *Power System Dynamics—Stability and Control*. Hyderabad, India: BS Publications, 2008.

[25] B. Sahoo and S. R. Samantaray, "System integrity protection scheme for enhancing backup protection of transmission lines," *IEEE Syst. J.*, early access, Aug. 20, 2020, doi: 10.1109/JSYST.2020.3013896.

[26] B. Taheri and M. Sedighizadeh, "Detection of power swing and prevention of mal-operation of distance relay using compressed sensing theory," *IET Gener., Transmiss. Distrib.*, vol. 14, no. 23, pp. 5558–5570, Dec. 2020, doi: 10.1049/iet-gtd.2020.0540.

[27] M. M. Eladany, A. A. Eldesouky, and A. A. Sallam, "Power system transient stability: An algorithm for assessment and enhancement based on catastrophe theory and FACTS devices," *IEEE Access*, vol. 6, pp. 26424–26437, 2018, doi: 10.1109/ACCESS.2018.2834906.

DOAA KHALIL IBRAHIM (Senior Member, IEEE) was born in Egypt, in December 1973. She received the M.Sc. and Ph.D. degrees in digital protection from Cairo University, Cairo, Egypt, in 2001 and 2005, respectively.

From 1996 to 2005, she was a Demonstrator and Research Assistant with Cairo University. In 2005, she became an Assistant Professor with Cairo University. In 2011, she became an Associate Professor with Cairo University. In December 2016, she became a Professor with Cairo University. From 2005 to 2008, she contributed to a World Bank Project in Higher Education Development in Egypt. From January 2010 to June 2013, she contributed as an expert in the Program of Continuous Improvement and Qualifying for Accreditation in Higher Education in Egypt. From July 2013 to November 2014, she contributed as an expert for the technical office of the Project Management Unit (PMU), Ministry of Higher Education, Egypt.

Dr. Ibrahim's research interests include digital protection of power systems, as well as utilization and generation of electric power, distributed generation, and renewable energy sources.

GHADA M. ABO-HAMAD received the B.S. and M.S. degrees in electrical power and machines from Cairo University, Giza, Egypt, in 2002 and 2009, respectively, where she is currently pursuing the Ph.D. degree in digital protection in electrical engineering.

From 2003 to 2009, she was a Designer Engineer with Consulting Engineering Company. From 2009 to 2012, she became a Teaching Assistant with the Industrial Education Collage, Automatic Control Department, Beni Suef University, Egypt. Since 2013, she has worked in Consultancy Engineering Companies, which design and supervise electric substations and distribution utilities projects. Her research interests include digital protection of power systems, as well as utilization and generation of electric power and flexible alternative-current transmission line technologies (FACT).

ESSAM EL-DIN M. ABOUL ZAHAB received the B.Sc. and M.Sc. degrees in electrical power and machines from Cairo University, Giza, Egypt, in 1970 and 1974, respectively, and the Ph.D. degree in electrical power from the University of Paul Sabatier, Toulouse, France, in 1979. He is currently a Professor with the Department of Electrical Power Engineering, Cairo University. He was an Instructor with the Department of Electrical Power and Machines, Cairo University, from 1970 to 1974. His research areas include protection systems, renewable energy, and power distribution. He is also the author or coauthor of many referenced journal and conference papers.

AHMED F. ZOBAA (Senior Member, IEEE) received the B.Sc. (Hons.), M.Sc., and Ph.D. degrees in electrical power and machines from Cairo University, Egypt, in 1992, 1997, and 2002, respectively, the Postgraduate degree in academic practice from the University of Exeter, U.K., in 2010, and the D.Sc. degree from Brunel University London, U.K., in 2017. He was an Instructor, from 1992 to 1997, a Teaching Assistant, from 1997 to 2002, and an Assistant Professor, from 2002 to 2007 with Cairo University, Egypt. From 2007 to 2010, he was a Senior Lecturer in renewable energy with the University of Exeter, U.K. From 2010 to 2019, he was a Senior Lecturer in power systems with Brunel University London, U.K. He is currently a Reader in electrical and power engineering with Brunel University London, U.K. His main areas of expertise include power quality, (marine) renewable energy, smart grids, energy efficiency, and lighting applications.

Dr. Zobaa is an Executive Editor for the *International Journal of Renewable Energy Technology*, an Executive Editor-in-Chief for *Technology and Economics of Smart Grids and Sustainable Energy*, and an Editor-in-Chief for the *International Journal of Electrical Engineering Education*. He is also an Editorial Board Member, Editor, Associate Editor, and Editorial Advisory Board Member for many international journals. He is a registered Chartered Engineer, Chartered Energy Engineer, European Engineer, and International Professional Engineer. He is also a registered member of the Engineering Council, UK, the Egypt Syndicate of Engineers, and the Egyptian Society of Engineers. He is a Senior Fellow of Higher Education Academy, U.K., Fellow of the Institution of Engineering and Technology, Energy Institute, U.K., Chartered Institution of Building Services Engineers, U.K., Institution of Mechanical Engineers, U.K., The Royal Society of Arts, U.K., The African Academy of Sciences, and Chartered Institute of Educational Assessors, U.K. He is a member of the International Solar Energy Society, The European Power Electronics and Drives Association, and the IEEE Standards Association.